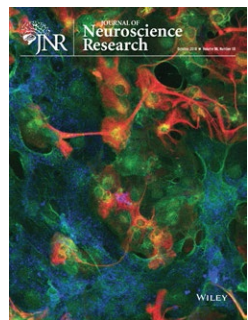




RESEARCH ARTICLE

Ultrastructural defects in stereocilia and tectorial membrane in aging mouse and human cochleae



Anwen Bullen¹ | Andrew Forge¹ | Anthony Wright¹ |
Guy P. Richardson² | Richard J. Goodyear² | Ruth Taylor¹

¹UCL Ear Institute, University College London, London, UK

²Sussex Neuroscience, School of Life Sciences, University of Sussex, Falmer, Brighton, UK

Correspondence

Anwen Bullen, UCL Ear Institute, University College London, London WC1X 8EE, UK.
Email: a.bullen@ucl.ac.uk

Funding information

Rosetrees Trust, Grant/Award Number: A528 JS15/M58-F1; Biotechnology and Biological Sciences Research Council, Grant/Award Number: BB/M00659X/1

Abstract

The aging cochlea is subjected to a number of pathological changes to play a role in the onset of age-related hearing loss (ARHL). Although ARHL has often been thought of as the result of the loss of hair cells, it is in fact a disorder with a complex etiology, arising from the changes to both the organ of Corti and its supporting structures. In this study, we examine two aging pathologies that have not been studied in detail despite their apparent prevalence; the fusion, elongation, and engulfment of cochlear inner hair cell stereocilia, and the changes that occur to the tectorial membrane (TM), a structure overlying the organ of Corti that modulates its physical properties in response to sound. Our work demonstrates that similar pathological changes occur in these two structures in the aging cochleae of both mice and humans, examines the ultrastructural changes that underlie stereociliary fusion, and identifies the lost TM components that lead to changes in membrane structure. We place these changes into the context of the wider pathology of the aging cochlea, and identify how they may be important in particular for understanding the more subtle hearing pathologies that precede auditory threshold loss in ARHL.

KEY WORDS

age-related hearing loss, cochlea, hair cell, hearing, RRID:SCR_002865, tectorin

1 | INTRODUCTION

Loss of hair cells from the organ of Corti occurs progressively with age in humans (Wright, 1982; Wright, Davis, Bredberg, Ulehlova, & Spencer, 1987), and is considered a major factor underlying age-related hearing loss (ARHL). Progressive age-related hair cell loss also occurs in the vestibular sensory epithelia of humans and is thought to underlie the balance dysfunction, dizziness, and vertigo that affects older people (Rauch, Velazquez-Villasenor, Dimitri, & Merchant, 2001). Age-related loss of cochlear hair cells and progressive hearing impairment with features similar to those of human

ARHL have been shown in a variety of animal species including mice, gerbils, rats, guinea pigs, and rhesus monkeys. Typically, outer hair cells (OHCs) which form part of the cochlear active amplifier but do not themselves transmit sound impulses to the auditory nerve suffer proportionally greater losses than inner hair cells (IHCs), which are responsible for the detection and transmission of sound stimuli to the brain. These patterns seem to be preserved across species (Coleman, 1976; Engle, Tinling, & Recanzone, 2013; Keithley & Feldman, 1982; Kusunoki et al., 2004; Tarnowski, Schmidt, Hellstrom, Lee, & Adams, 1991; Wright, 1984; Wright et al., 1987). ARHL is often considered to be characterized by increase in auditory thresholds initially to sounds of high frequency, and spreading progressively to include successively lower frequency hearing that corresponds to hair cell loss in a pattern, initiated and most extreme

Edited by Lisa Nolan. Reviewed by Gregory Frolenkov, Peter Thorne, and Bo Zhao.

The peer review history for this article is available at <https://publons.com/publon/10.1002/jnr.24556>.

in the basal end of the cochlea and progressively encompassing more apical regions. However, a comprehensive study of ARHL of the UK population (Davis, 1995) showed that reduction in auditory thresholds at the lowest frequencies as well as high frequencies, and a similarly extensive study of hair cell losses with aging in humans (Wright, 1982) revealed a corresponding progressive loss of hair cells from the cochlear apex as well as from the base (Legan et al., 2014; Wright, 1982). The age-related death of hair cells has been associated with mitochondrial dysfunction, free radical production, and stimulation of apoptosis pathways (Yamasoba et al., 2007).

Correlated with hair cell loss is the retraction and loss of spiral ganglion afferent nerve fibers, which synapse with IHCs (Bao & Ohlemiller, 2010), but recently it has been recognized that loss of afferent synaptic connections to IHCs may progress in the absence of any obvious hair cell loss or injury and without causing any recordable increase (decrement) in auditory thresholds. Such "synaptopathy" is now considered to be an important early age-related pathology. Evidence of this phenomenon has been identified in both humans and animals (Gleich, Semmler, & Strutz, 2016; Kujawa & Liberman, 2015; Parthasarathy & Kujawa, 2018; Sergeyenko, Lall, Liberman, & Kujawa, 2013; Wu et al., 2018) and the neuronal loss may be selective, affecting first fibers with low thresholds and high spontaneous rates of activity (Schmiedt, Mills, & Boettcher, 1996). These losses have been suggested to correlate with some of the early and more subtle signs of ARHL that precede auditory threshold shifts such as difficulties with discriminating speech in noise (Parthasarathy & Kujawa, 2018).

Changes also occur during aging to the structures that surround and support the function of the organ of Corti, particularly the stria vascularis. This pathology manifests as structural changes, including a thinning of the stria identified in both humans (Suzuki et al., 2006) and animals (Ichimiya, Suzuki, & Mogi, 2000). At the ultrastructural and molecular level, marginal cells of the stria vascularis show mitochondrial degradation (Thomopoulos, Spicer, Gratton, & Schulte, 1997), retraction of their interdigitating processes (Gratton, Schmiedt, & Schulte, 1996), and a reduction in the expression of the sodium-potassium pump that is vital for maintaining the high positive "endocochlear potential" in the cochlear fluid that bathes the apical surface of the organ of Corti and is vital for its function (Schmiedt, 1996). Age-related loss of cells of the spiral ligament that may impact cochlear homeostasis has also been noted (Hequembourg & Liberman, 2001).

Aging is a multifactorial process, affecting various tissues and cells in different ways, so it is unsurprising that there are deleterious effects at a variety of sites in the inner ear which together may contribute to the recordable age-related functional deficits in hearing and balance. In this paper we present data from our aging studies in mice and humans, showing the effects of aging at two crucial sites that have not been examined in detail previously: stereocilia and the tectorial membrane (TM). Defects to these structures are likely to affect the precision of sound encoding within the organ of Corti, and are potential candidates for the causes of ARHL that occur prior to the loss of auditory thresholds.

Significance

Understanding the etiology of age-related hearing loss (ARHL) is vital to effective prevention and therapy. Potential therapeutic approaches often focus on correcting a single or narrow range of pathological changes (e.g., degeneration of hair cells or afferent synapses) but do not address other cochlear pathologies. The significance of this work is the detailed description of additional pathological changes that have been poorly appreciated in the literature to date, but are likely to have significant effects on hearing in aging. This work will help to inform a more rounded picture of the causes of ARHL, and encourage broader approaches to prevention and therapy.

2 | METHODS AND MATERIALS

2.1 | Animals

Inner ear tissues were obtained from male CBA/Ca mice aged between 10 weeks and 32 months. A single sex of mice was used to enable fair comparison of all samples, as there are known differences between sexes in the severity of ARHL (Guimaraes, Zhu, Cannon, Kim, & Frisina, 2004). With the exception of electron tomography, which was performed on only a small number of representative samples, at least six animals at 6–8, 12, 17–19, 23–26, and 30–32 months were examined, one ear from each animal prepared by one of the processing procedures outlined below and the other for a different one. All procedures involving the use of animals were approved by UCL Animal Ethics committee and performed with authority of a project license from the British Home Office.

Animals were killed by carbon dioxide inhalation according to schedule 1 procedures. Auditory bullae were isolated and the inner ear tissues fixed by direct perfusion. Fixative was gently injected via an opening at the apex of the cochlea, through a rupture of the round window and opening the oval window. For scanning and transmission electron microscopy, the fixative was 2.5% glutaraldehyde in 0.1 M cacodylate buffer with 3 mM CaCl₂, and for immunolabeling was 4% paraformaldehyde in phosphate-buffered saline (PBS). The intact cochleae were decalcified in 4% EDTA for 48 hr at 4°C. Both left and right ears were used for examination, and this was selected randomly.

2.2 | Auditory brainstem responses

Male mice were anesthetized using intraperitoneal ketamine (Vetalar™; Pfizer UK Limited, 0.01 ml/g of 10 mg/ml) and medetomidine (Domitor, Orion Corporation, Finland, 0.005 ml/g of 0.1 mg/ml) and placed in a soundproof booth (Industrial Acoustic Company Ltd). Body temperature of the animals was maintained using a

homeothermic blanket maintained at 37°C. Subdermal needle electrodes (Rochester Electro-Medical) were inserted at the vertex (active), mastoid (reference) and with the ground needle electrode in the hind leg. Recordings were obtained using TDT system 3 equipment and software (Tucker-Davis Tech., Alachua, FL). Click stimuli and tone pips at 8,122,432, and 40 kHz were presented at 80 dB SPL and then in decrements of 10 dB, and from the responses recorded the auditory threshold was determined by the lowest sound pressure level at which the auditory brainstem response (ABR) waveform could be recognized. If no response was detected at the maximum stimulus level (80 dB), a threshold of 90 dB was recorded for subsequent graphical representation.

2.3 | Statistics

As ABRs were performed on the same groups of male mice as they aged (with animals killed for cochleae analysis at each time point). ABR data were compared using a repeated measures ANOVA, with Greenhouse-Geisser correction where the data violated the sphericity assumption. Sphericity was determined by Mauchly's test. *p* value and corrected degrees of freedom are reported. Calculations were carried out in SPSS (SPSS version 26, IBM, New York, USA, RRID:SCR_002865).

2.4 | Transmission electron microscopy and electron tomography of mouse inner ears

Fixed, decalcified cochleae were postfixed and stained with osmium tetroxide and uranyl acetate, before dehydrating through a graded series of ethanols and embedding in an Epon resin. Samples for electron tomography were incubated in a solution of 0.1% tannic acid in 0.1 M cacodylate buffer before postfixation and staining.

Sections of the entire intact inner ear were cut at several different depths through the cochlea and sections for examination were collected at each of these depths. Following initial examination by light microscopy of 1 µm thick sections stained with toluidine blue, for routine TEM, serial 100 nm thick sections were collected at each depth through the cochlea and placed on uncoated copper grids, stained with lead citrate and uranyl acetate and imaged at 80 kV in a JEOL JEM-1200 EX II transmission electron microscope (TEM). For electron tomography, 200 nm sections on formvar-carbon-coated copper grids were stained similarly and 10 nm gold particles were applied as fiducial markers. Sections were imaged in a JEOL JEM-2100 microscope operating at 200 kV. Dual axis tomogram tilt series were collected at 1° increments for an axis of -60 to +60° and a pixel size of 0.371 nm.

2.5 | Electron tomography reconstruction

Reconstruction of electron tomography datasets was carried out using etomo, part of the IMOD program suite (Kremer, Mastronarde,

& McIntosh, 1996). Tomograms were reconstructed using weighted back projection with an applied SIRT-like filter equal to five iterations. Segmentation was carried out using the 3DMOD program. For drawn objects contours were manually drawn or traced using assisted (livewire) segmentation at Z-axis intervals of 1.85 nm. Microtubules were modeled using point modeling with representative tubes. Isosurface rendering was carried out using the isosurface tool included in the IMOD package and were rendered across the complete Z-axis of the reconstructed images (excluding surface gold particles).

2.6 | Scanning electron microscopy of mouse inner ears

Organs of Corti and utricular maculae and cristae were dissected from the fixed, decalcified inner ears, postfixed in OsO₄, and processed through the thiocarbohydrazide-Os-repeated procedure (Davies & Forge, 1987) before dehydrating in an ethanol series, critical point drying, and sputter coating with platinum. Samples were examined in a JEOL 6700F SEM operating at 5 kV by secondary electron detection.

2.7 | Scanning electron microscopy of resin sections

Samples were prepared as for transmission electron microscopy. Sections of 100 nm thickness were collected on Kapton tape in an automatic tape ultramicrotome (RMC, USA) as described previously (Bullen, 2019). Sections on tape were mounted on conductive carbon tape on silicon discs, coated with 12 nm of carbon and examined in a JEOL 6700F SEM operating at 5 kV by backscattered electron detection. Image montages (~100 images) were automatically collected, stitched, and normalized by SEM Supporter software (System In Frontier, Japan).

2.8 | Immunohistochemical labeling of frozen sections of mouse ears

Paraformaldehyde fixed, decalcified intact cochleae were incubated overnight at 4°C in 30% sucrose solution, embedded in low-temperature setting agarose (Sigma), oriented and mounted on specimen-support stubs using OCT and then frozen. Frozen sections were cut at 15 µm and collected on polylysine-coated slides (Polysine™, VWR). Tissue was permeabilized in 0.5% Triton in PBS for 20 min and the sections then incubated in blocking solution (10% goat serum in PBS with 0.15% Triton X-100). Tissue was incubated in primary antibody overnight at 4°C rinsed thoroughly in several changes of PBS and then incubated with appropriate secondary antibody conjugated to a fluorophore for 90 min at room temperature. A fluorescent phalloidin conjugate was added at 1 µg/ml to the secondary antibody solution. Samples were mounted on to slides using Vectashield with DAPI (Vector Laboratories) to label nuclei and examined and imaged

on a Zeiss AxioImager widefield microscope. The primary antibodies used were a rabbit polyclonal to mouse α -tectorin (TECTA) (Legan et al., 2014), a rabbit polyclonal to chick β -tectorin (TECTB) (R7, Knipper et al. (2001), and a rabbit polyclonal to mouse carcinoma and embryonic antigen-related cell adhesion molecule 16 (CEACAM16) (Zheng et al., 2011)).

2.9 | Human tissue: Scanning electron microscopy of organ of Corti

From an archive of samples prepared for *electron microscopy* during the 1980s, organs of Corti from individuals with no known auditory pathology prior to death were re-examined. The archive contained 30 samples; 22 male and 8 female; mean age 56.8; age range 17–81. Female samples: mean age 55.3, age range 26–76. Male samples: mean age 56.5, age range 17–81. Procedures were performed in accordance with the UK legislation in force at the time; in the UK in the 1980s, the standard hospital postmortem form allowed for removal of tissues other than for the purposes of transplantation provided the relatives' consent had been obtained. Appropriate consent was obtained for all samples used in this study. Within 40 min of death, a tympano-metral flap was raised and the stapes removed. An angulated blunt needle was used to perforate the round window membrane and 5 ml of 2.5% glutaraldehyde/2% formaldehyde in 0.1 M sodium cacodylate buffer with 2 mM calcium chloride at pH 7.25 was gently perfused through the cochlea. The two windows were sealed with plasticine. A small cube of the temporal bone containing the labyrinth was then removed and placed in fresh fixative. The delay between death and removal of the labyrinth was never more than eighteen 18 hr. The bones were then reperfused with the glutaraldehyde/formaldehyde fixative and left for 24 hr before reperfusion with buffer then perfusion with 1% OsO₄. The two windows were again sealed and the specimen was left for 2 hr. The osmium was washed out with buffer then 50% ethanol and the specimen was dissected under 50% alcohol to reveal the membranous labyrinth. The stria vascularis was removed as was the TM. The spiral lamina was dissected in segments from apex to base; photographed then stored in 70% ethanol. The specimens were dehydrated in an ethanol series before critical point drying from liquid CO₂. The specimens were mounted on stubs using Araldite glue and then sputter coated with gold and palladium. Reexamination was of images taken after the original processing of the samples, or reexamination of samples as required. Reexamination of the samples was carried out on a JEOL 6700F SEM, operating at 5 kV using secondary electron detection. The samples did not show significant degradation when compared to archive images.

2.10 | Human temporal bone sections

Hematoxylin-eosin stained serial sections were taken from the archive of human temporal bone sections at the UCL Ear Institute.

Accompanying medical notes were used to identify the samples from patients whose recorded auditory deficits were ascribed to "presbycusis." Three male subjects with a presbycusis diagnosis were selected and examined along with three age and sex-matched controls with no reported hearing deficit.

3 | RESULTS

3.1 | Stereociliary fusion, elongation, and internalization are common features of aging in both the mouse and human inner ear

CBA/Ca mice, unlike some other mouse strains, do not exhibit an accelerated loss of hearing with age. Figure 1a shows ABR as a measure of hearing in a cohort of aging CBA/Ca mice. The mice show loss of threshold with increasing age, particularly evident at the low-frequency (apical) and the high-frequency (basal) ends of the cochlea. The organs of Corti of 6–8 months old mice appeared normal—there was no obvious hair cell loss and hair bundles on both IHCs and OHCs appeared intact (Figure 1b,c). At approximately 12 months of age, there was no significant loss of OHCs. The hair bundles of IHCs scattered along the organ of Corti showed fusion of stereocilia (Figure 1d). OHC hair bundles did not show fusion defects. At 18 and 24 months and later, although there was no obvious significant loss of IHCs, even at 30 months of age, fused stereocilia persisted and became more prevalent (Figure 1e–l). Fusions involved a variable number of stereocilia from doublets to an encompassing of almost the entire stereociliary bundle and appeared to be initiated in the longest row (Figure 1j,l). Stereocilia were also often significantly elongated above the height of the longest stereocilia of the apparently unaffected hair bundles on adjacent IHCs (Figure 1k). Such "giant" stereocilia became more numerous and more elongated with age. Quantification of samples where a large region of the organ of Corti was available at appropriate angles showed that at 6 months there were no fused or giant stereocilia observed, and no IHC loss ($n = 4$ mice). By 12 months, 8% of total IHCs had evidence of stereociliary fusion, but no giant stereocilia were observed ($n = 3$ mice). By 24 months, 20% of total IHCs showed stereociliary fusion, and of these fusions 30% contained giant stereocilia. Giant stereocilia were only present on cells that also showed evidence of fusion. Giant stereocilia were also twice as common at the apical end of the cochlea as they were at the base ($n = 5$ mice). These observations indicate that following fusion of their stereocilia, IHCs survive intact and the fused stereocilia continue to elongate. With increased age, there was increasing loss of OHCs, but fusion of OHC stereocilia similar to that observed in IHC was not seen, suggesting that at least in OHC, stereociliary fusion is not an indicator of hair cell degeneration and incipient death.

Samples of the human organ of Corti from a 26 years old individual showed intact, normal appearing hair bundles on IHCs and OHCs across the cochlea (Figure 2a–c). However in organs of Corti from the older individuals (aged between 60 and 70), in addition to the expected loss of hair cells, fused and elongated stereocilia and

evidence of their internalization was apparent on some scattered IHCs. Stereocilia become internalized into the apical cytoplasm, apparently through fusion of the stereociliary membrane with the

apical plasma membrane (Figure 2d–h insets and red arrows). Unlike in the mouse, giant, fused stereocilia were very occasionally evident on OHCs (Figure 2g). A comparison between mouse and human

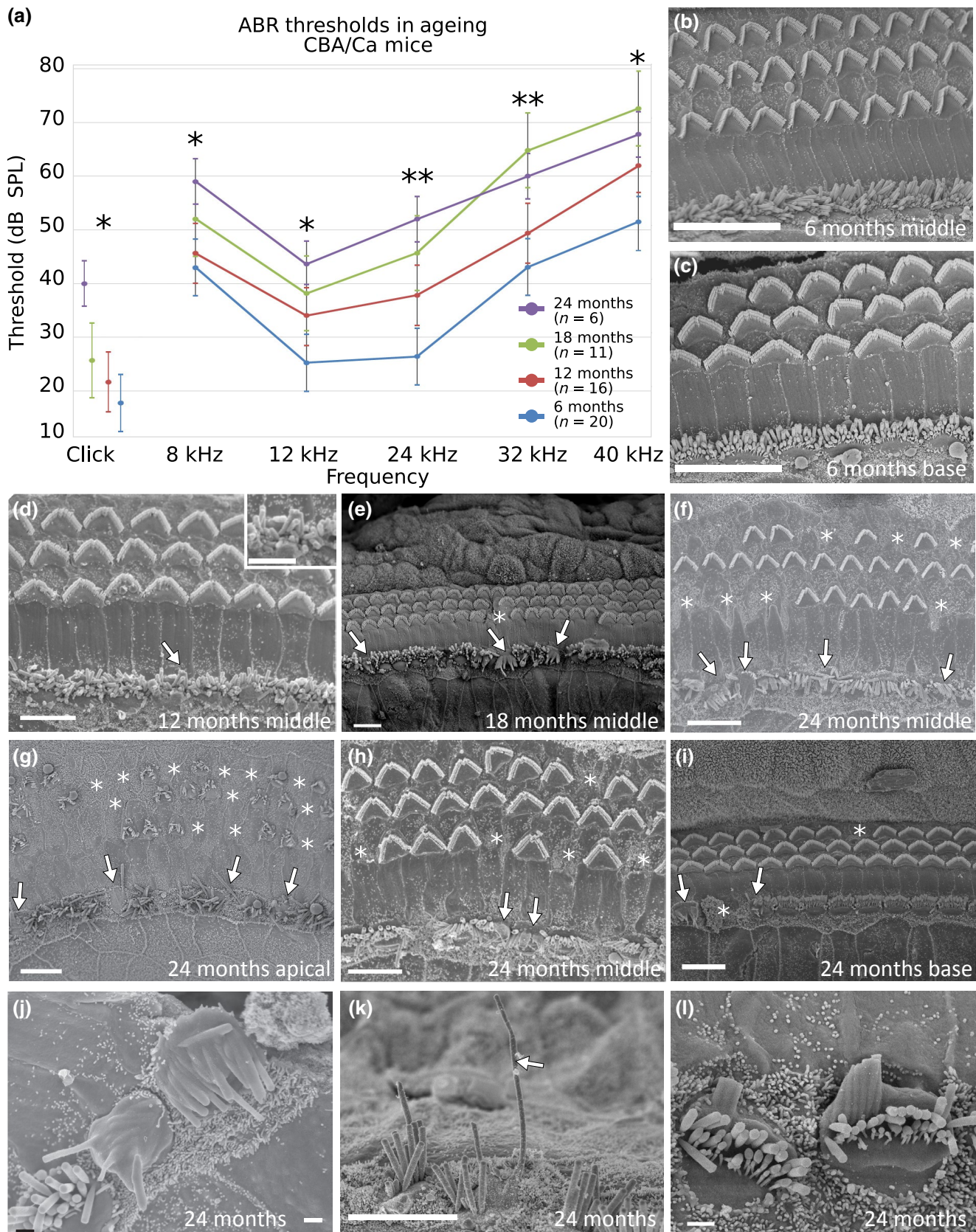


FIGURE 1 Stereocilia fusion, elongation, and internalization in aging mice cochleae. (a) ABR thresholds in an aging cohort of CBA/Ca mice. Threshold increases at both the high and low-frequency regions are evident at 18 and 24 months. Error bars represent standard error of the mean (SEM). ** = p values ≤ 0.001 . Animals per group: 6 months ($n = 20$), 12 months ($n = 16$), 18 months ($n = 11$), and 24 months ($n = 6$). p values for repeated measures ANOVA (Click stimuli $p = 0.01$, $df = 1,416$. Tone stimuli: 8 kHz $p = 0.042$, $df = 3$. 12 kHz $p = 0.025$, $df = 3$. 24 kHz $p \leq 0.001$, $df = 3$. $p \leq 0.001$, $df = 3$. 32 kHz $p \leq 0.001$, $df = 3$. 40 kHz $p = 0.004$, $df = 3$.) (b) Middle coil and (c) Basal coil from a 6 months mouse. No evidence of inner or OHC damage is present. (d-f) Middle coil in (d) 12 months, (e) 18 months, and (f) 24 months mice. Stereociliary fusions and internalization are present in all three (white arrows); both fusion and lost hair cells (*) are more prevalent at older ages. Boxed region in (d) represents an enlargement of the stereociliary fusion defined by the arrow. (g-i) (g) apical, (h) middle, and (i) basal coils of mouse cochleae at 24 months of age. Fusions and hair cell loss are most severe in the apical region. (j-l) Stereociliary defects in 24 months mice. (j) Severe stereociliary fusions and internalization. (k) Elongation of stereocilium. (l) Fusion across longest stereociliary row. Scale bars: (b-i and k) 10 μ m, (j and l) 1 μ m

IHCs shows the similar patterns of stereociliary fusion observed between the two species (Figure 2h,i).

As we have previously reported (Taylor et al., 2015), fusion and elongation of stereocilia with aging is also a feature of hair cells in vestibular sensory epithelia. In mice, fusion of stereocilia in the absence of any obvious hair cell loss was evident in utricular maculae and cristae by 12–18 months (Figure 3a). By 24 months, loss of hair cells was evident by their reduced density and patches where hair cells were entirely absent, while on remaining hair cells there was a significant elongation of fused stereocilia (Figure 3b,c). The fusion involved not only the stereocilia but the kinocilium also became incorporated into the fused hair bundle. Similar fusion and elongation of stereocilia incorporating the kinocilium was also observed in the utricular maculae and cristae of older people (Figure 3d,e) (Taylor et al., 2015). The presence of “giant” fused stereocilia in IHCs of the organ of Corti and hair cells of vestibular organs indicates that the addition of actin monomers to the stereocilia continues even after they are fused.

Internalization of the stereocilia was more clearly defined in sections of IHCs prepared for TEM, where seemingly intact stereociliary actin-filament bundles were enclosed beneath the apical plasma membrane, displacing the cuticular plate which became detached from the membrane (Figure 4). Thin sections also showed that the cell bodies of IHCs with fused, and internalized and/or giant stereocilia were intact with no obvious other signs of damage or degeneration (Figure 4a,b,d,e), and that afferent terminals synapsing with these cells were mostly intact and not swollen (Figure 4a,d). However, there were vesicles present in the region of the fusion; these vesicles appeared to be double-membraned, and in some cases to have vesicular contents suggesting they may represent autophagic vesicles (Figure 4d,e).

3.2 | Actin bundles do not fuse after stereociliary fusion

Stereociliary fusion could have several potential effects on the stereocilia structure, from fusion of only the stereociliary membranes to a breakdown of the organization of the actin bundles. TEM sections through fused stereocilia appear to show that the actin bundles of the stereocilia remain intact despite the fusion (Figure 4a,b). The densely packed actin filaments that normally form the rootlet are present, although they appear to be incorporated higher up the shaft of the

stereocilium than we would normally expect, perhaps evidence of continued but dysregulated growth of the stereocilia. This is consistent with the observation from SEM data that fused bundles continue to elongate, indicating that actin structures are being maintained by the cell, although their growth may have become dysregulated. The plasma membranes of the stereocilia do appear to fuse. Examination of fused stereocilia from a 1-year old mouse IHCs by electron tomography shows similarly that the actin structures (visualized by isosurface rendering across a 200 nm section of stereocilia) do not appear to be disrupted by the fusion (Figure 4f,g). Stereociliary rootlets are still clearly visible and well-formed, and dividing lines between the actin bundles of different stereocilia are still visible, suggesting the bundles themselves have remained separated, and appear similar to neighboring unfused stereocilia (Figure 4f-h(ii),(iv),i(i)). However, there is a clear fusion between the membranes of several stereocilia (Figure 4f,h(i)). In addition, tomographic reconstruction suggests that other cytoskeletal components are also present in the fusion. Unfused IHC stereocilia are rooted into the cuticular plate, and little space exists in between the cuticular plate and cell membrane. However in both the tomogram and TEM sections, a space has developed between the cuticular plate and cell membrane in the region of the fusion (Figure 4a,b,f-j). This space is occupied by the microtubule-like elements (red tubes) (Figure 4g,j) as well as membranous structures (membrane cisterns) that could be divided into several different types—those without visible contents which were either greater than 100 nm in diameter (purple) (Figure 4g,j) or less than 100 nm in diameter (blue), those with cytoplasmic contents (orange), and tubular cisternae (white) (Figure 4f,h(iii)) (Supporting Information Movie S1). The microtubule elements appear to be reaching into the body of the stereociliary fusion (Figure 4j(iii)).

3.3 | The TM undergoes significant structural changes with aging

Along with fusion of IHC stereocilia, a second remarkably consistent feature of the aging mouse cochleae was a progressive degeneration of the TM. The normal characteristic appearance of the TM as described in detail elsewhere (Goodyear & Richardson, 2002, 2018; Hasko & Richardson, 1988) was evident throughout the length of the cochleae in 6–8 months old mice. In sections for light microscopy stained with toluidine blue, the TM was characteristically shaped, overlying the organ of Corti and attached to the spiral limbus on its medial side, and evenly stained (Figure 5a). The sections showed

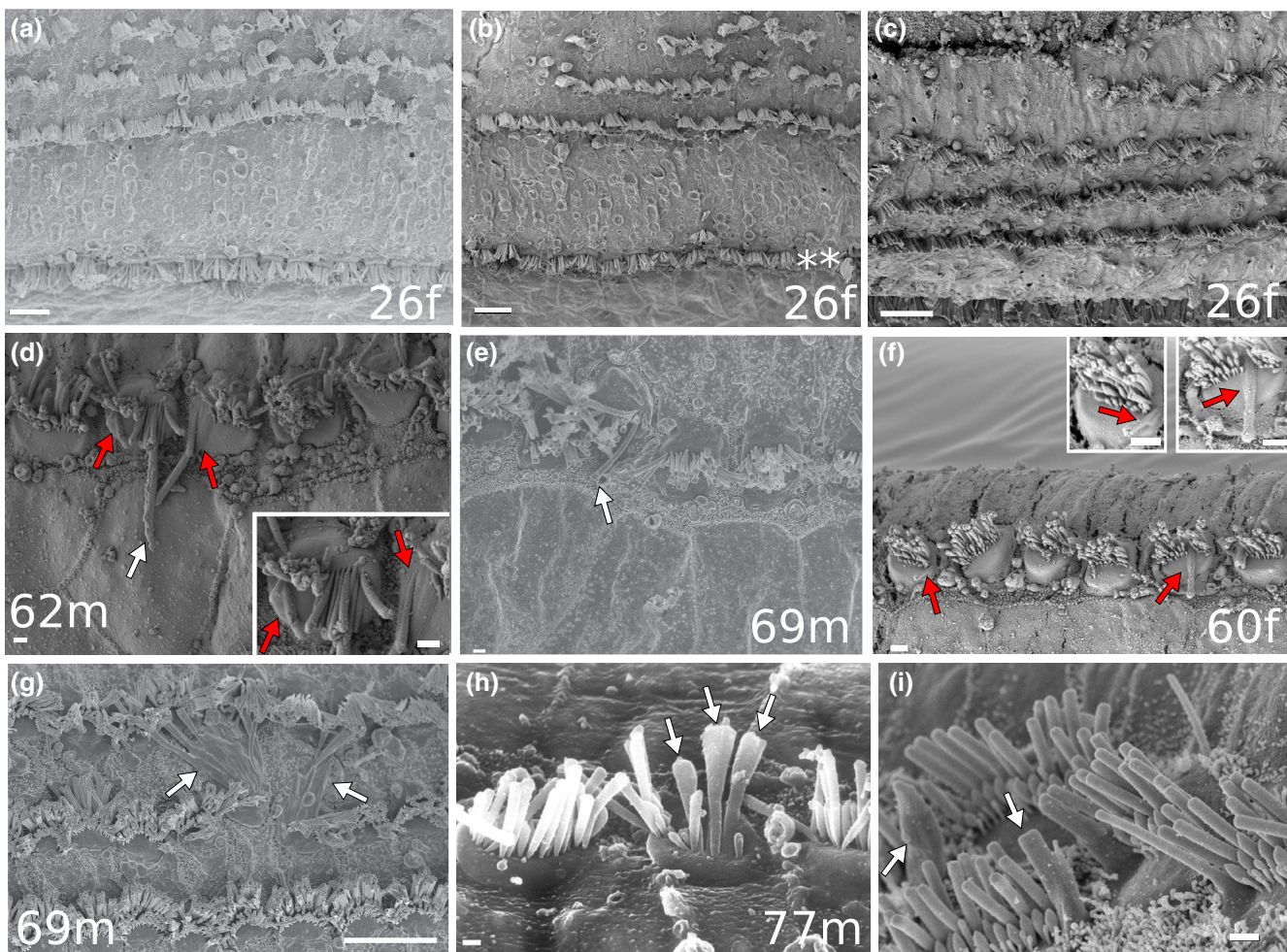


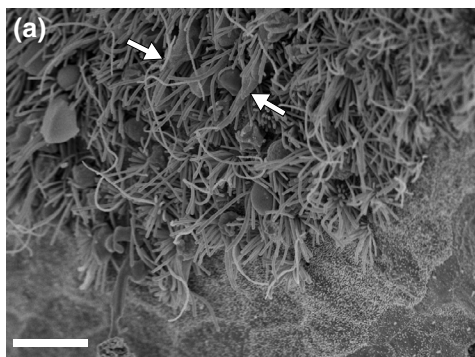
FIGURE 2 Stereocilia fusion, elongation, and internalization in aged-human cochleae. All cochleae were from people who had no recorded hearing loss at time of death. (a–c) Apical middle and basal cochlear turns from 26 years old female. Irregularity in the rows, presence of a 4th row of OHCs in (c), and supernumerary OHCs and IHCs are evident, these are characteristic of the normal human organ of Corti. Scattered loss of IHCs is indicated by (*), but stereociliary defects were not observed. (d–i) Evidence of fusion and elongation (white arrows) and internalization (red arrows and insets) in (d) a 62 years old male, (e) a 69 years old male, and (f) a 60 years old female. (g) Fusion, elongation, and engulfment of OHC stereocilia in a 69 years old male. Fusion of OHC stereocilia was not observed in mice. (h and i) Comparison of fused, elongated stereocilia in human (h, 77 years old male) and mouse (i, 30 months). Scale bars: a–c and g = 10 μ m, d, e, h–i = 1 μ m (inset 1 μ m), f = 2 μ m (insets 2 μ m)

a core composed of parallel, radially oriented quite-closely packed collagen fibrils embedded within a uniform matrix, with denser regions on the upper surface, at the tip and on the lower surface, particularly in the ridge comprising the Hensen's stripe (Goodyear & Richardson, 2002). Subsequently, there was a progressive degeneration of the TM that was first apparent in the apical coil from about 12–18 months then proceeded with age into the basal coil by 24–30 months (Figure 5b,c). There was a decrease in the density of toluidine blue staining of the core of the TM and also there were changes in shape, initially a swelling and then often a thinning. As degeneration of the TM proceeded into the basal coil, it often became detached from the spiral limbus and the detached membrane rest against Reissner's membrane, this detachment also proceeded in an apex to base direction (Figure 5c). The degeneration observed did not appear due to fixation artifacts in the TM. All TMs examined from 6–8 months mice had the same appearance as that shown here

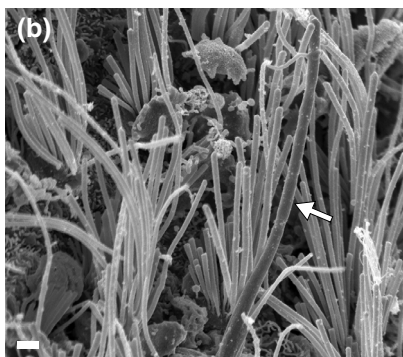
(including many 6–8 months mice we have examined in the past that were not included in this study). The degeneration of the TM was also remarkably consistent in all aging samples, including aging mice we have examined for other studies. In addition, no other significant fixation artifacts were apparent in the organ of Cortis of the mice examined. This consistency and lack of associated fixation artifacts strongly suggests these effects are not due to fixation.

3.4 | Changes in TM are present in the cochleae of some humans with presbycusis

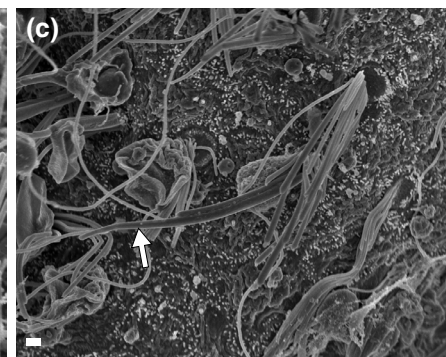
The TM of an individual (55 years) with no known hearing deficit (Figure 5d) showed similar structure to that of young mice. However, abnormalities of the TM were observed in sections of the temporal bones from two out of the three individuals whose clinical notes

Mouse utricular macula

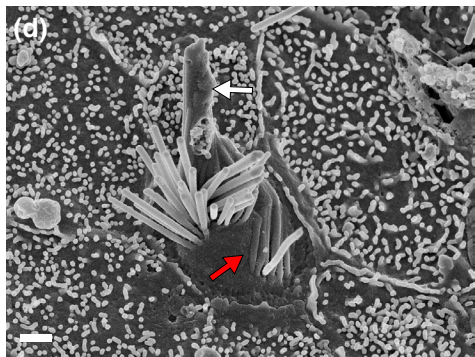
18 months



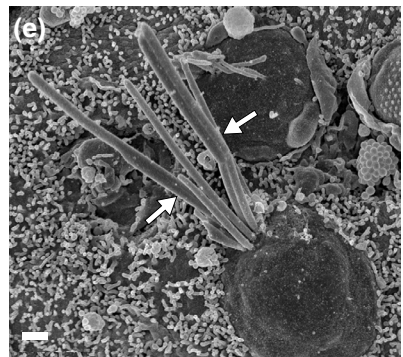
24 months

Mouse crista

24 months

Human utricular macula

Male, 70 years



Male, 65 years

FIGURE 3 Stereocilia fusion, elongation, and internalization in aged mouse and human vestibular tissue. (a) Mouse utricular macula at 18 months. (b) Mouse utricular macula at 24 months. (c) Mouse crista at 24 months. (d,e) Human utricular macula: Male, 70 years (d); Male 65 (e). Arrows indicate fused stereocilia, elongation of stereocilia, and internalization of stereocilia. In mouse, fusion of stereocilia is apparent before any significant hair cell loss, as indicated by close packing and high density of hair cells (a). Fused and elongated stereocilia persist in utricular maculae (b) and cristae (c) for at least 24 months by which time there is also a reduced density of hair cells. Internalization of stereocilia (red arrows) (d) as well as stereociliary fusion (e) are also features of the utricular macula in aging humans. Scale bars: (a) 10 μ m, (b–e) 1 μ m

attributed a hearing loss to “presbycusis.” In a specimen from an 81 years old male, the TM was remarkably thinner than normal (Figure 5e). In the apical coil it was detached from the spiral limbus and attached to Reissner’s membrane. In the middle coil it was displaced toward Reissner’s membrane but not attached to it (Figure 5e). In a specimen from a 71 years old male, in the apical coil the TM was thinned and attached to Reissner’s membrane, while in the basal coil it was distorted in shape but seemingly not attached to Reissner’s membrane, although extracellular material exists between the two (Figure 5f).

3.5 | Loss of matrix components in aged TM

TEM and electron tomography reconstructions revealed there was loss of the matrix components from the core of the TM (Figure 6), but loss of collagen fibrils was also evident. The initial progression of degeneration of TM proceeded prior to any hair cell loss. Both IHCs and OHCs were present and apparently intact in the organ of Corti beneath degenerating TM. Degenerating TM was also evident in regions

where there was no obvious significant loss of spiral ganglion neurons (Figure 6a,b). The TM often appeared to become “motheaten” with not only loss of matrix from the core but also apparent discontinuities in the collagen fibrillary structure. In some of the oldest animals examined, 24–30 months, the core of the TM was almost entirely lost with only the initially dense fibrillary complexes on the upper and lower surface and at the tip remaining (Figure 6c–f). Electron tomography was carried out on a younger (1 year) specimen to ensure there would still be matrix material available to examine. Isosurface reconstruction showed that even by 1 year, the matrix material has begun to thin, leaving gaps in the membrane structure (Figure 6g,h). This was evidenced by an overall reduction in the proportion of the reconstruction volume containing TM components from 35% to 30%.

3.6 | Degeneration of TM is associated with loss of tectorins

The major non-collagenous components of the TM are the glycoproteins TECTA, TECTB, CEACAM16, and otogelin (Goodyear &

Richardson, 2002; Zheng et al., 2011). To establish whether the loss of protein constituents of the TM was the cause of the structural degeneration observed, immunohistochemistry for TECTA,

TECTB, and CEACAM16 was performed. In the cochleae of mice at 6–8 months, antibodies to TECTA (not shown) and TECTB labeled the TM equally intensely in all turns. The apical turn, which was the

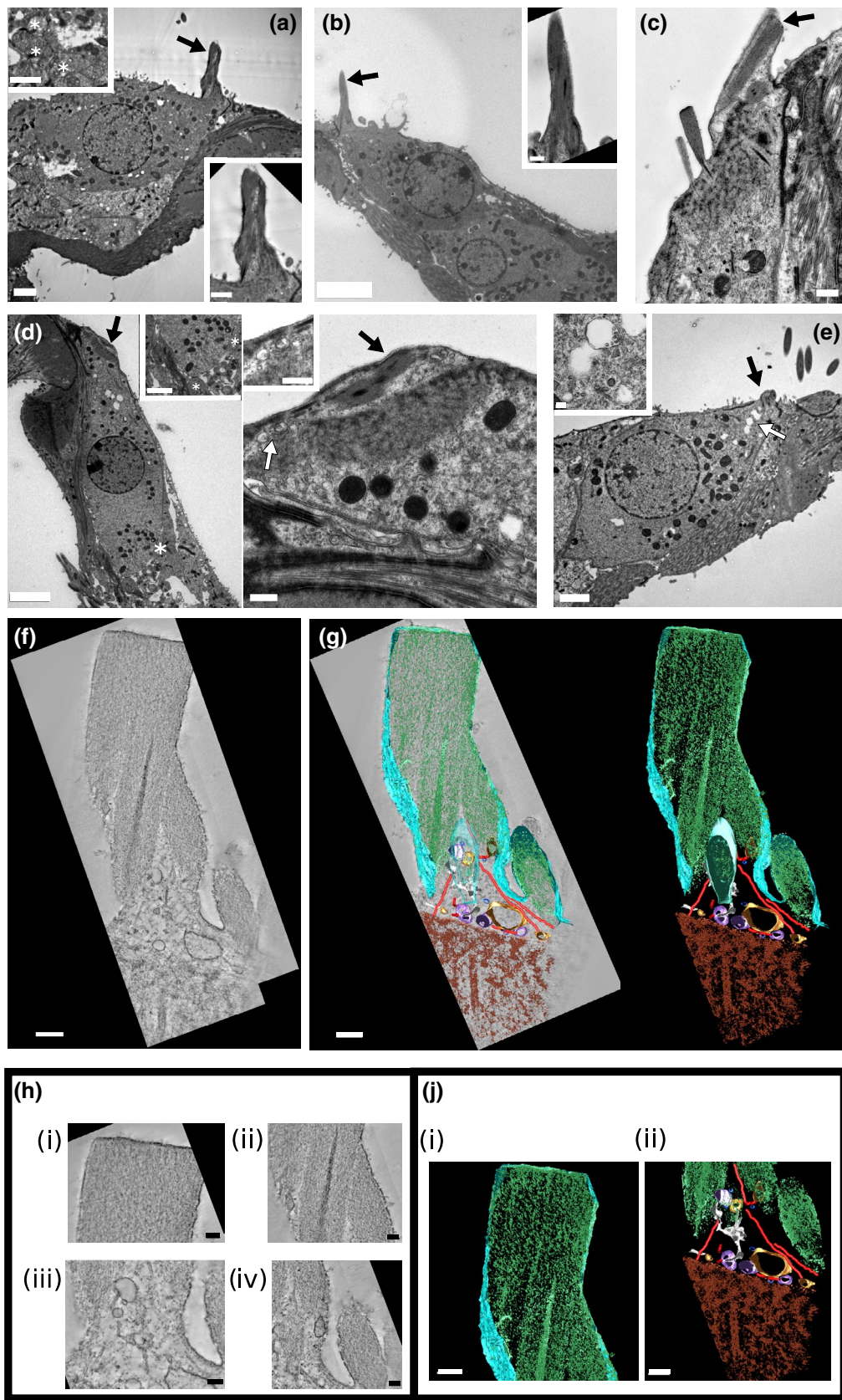


FIGURE 4 Cross-sectional examination of fused stereocilia bundles. (a–e) TEM cross sections of IHCs carrying fused or internalized stereocilia. (a–b) Stereociliary fusions (black arrows) on IHCs from mice aged 18 months. Despite the fusions, the cell bodies appear normal and surrounding structures are not apparently impaired. Asterisks on enlarged insets in a and d indicate intact afferent terminals synapsing with the IHCs. (c) Internalization of stereocilia by the apical membrane (black arrow), 24 months mouse. (d–e) Internalization of stereocilia (black arrows) in (d) 30 months and (e) 24 months mouse. In both cases, the cell bodies and surrounding structures do not appear damaged. Insets show vesicles present in the cytoplasm near the sites of internalization. These vesicles appear double-walled, and to have contents. (f) Central section of tomographic reconstruction of fused IHC stereocilia. (g) Segmented reconstruction of stereociliary fusion. Manual segmentation was used for membranes and microtubules, actin filaments were rendered by isosurface rendering. Light blue = cell membrane. Green = Stereociliary actin. Red = Microtubules. Purple and Blue = Membranous spheres without apparent contents (large and small respectively). Orange = membranous spheres with cytoplasmic contents. White = tubular cisternae. Brown = Isosurface rendering of cuticular plate. (h) Enlarged regions of central slice of tomographic reconstruction showing (i) stereociliary fusion tip with continuous membrane and actin filaments. (ii) Central shafts of stereociliary fusion with gaps between adjacent stereocilia and actin bundles, membrane fusion, and central stereociliary rootlet. (iii) Cytoskeletal elements and membranous objects at the base of the stereociliary fusion. (iv) Individual stereocilium not included in fusion, showing similar actin pattern. (j) Enlargements from segmentation showing (i) pattern of actin isosurface for complete 3D reconstruction of stereociliary fusion. (ii) Cytoskeletal and membrane components between fusion and cuticular plate. Scale bars: a = 2 μ m (inset) = 1 μ m, b = 5 μ m (inset = 500 nm), c = 500 nm, d (left) = 5 μ m (right) = 500 nm (inset) = 500 nm, e = 2 μ m, (inset) = 200 nm, f–g = 250 nm, h (i–iv) = 100 nm, j (i, ii) = 200 nm. For model rotations please see Supporting Information Movie S1

first to show degradation in older mice, is shown in Figure 7a. At 18–19 months, the TM in the apical coil showed reduced labeling intensity in the core, but labeling still outlined the periphery and the labeling intensity in lower turns was greater and similar to that in the 6 months old mice for both TECTA and TECTB (Figure 7b,c). Progressively with age, reduction in labeling intensity of the TM proceeded into lower coils and to the basal coil by 24–30 months (Figure 7b,c). The loss of both TECTA and TECTB showed the same pattern of central to periphery loss and the base to apex gradient as seen in the cochleae of mice by light and electron imaging. The third matrix component CEACAM16, necessary for the formation of the striated sheet, showed a similar pattern of loss (Figure 7d). Therefore, the loss of TM density observed is likely due at least in part to the loss of these proteins from the TM representing a failure to maintain the matrix in older animals.

4 | DISCUSSION

Understanding the multifactorial nature of ARHL is important to any form of the effective treatment for presbycusis. Although traditionally hearing loss has been measured in terms of the loss of pure tone thresholds alone, more recently it has become clear that a variety of other changes to hearing occur before measurable threshold loss (Barbee et al., 2018). These deficits, known colloquially as “hidden hearing loss,” have been attributed largely to synaptopathies affecting a subpopulation of the afferent nerves contacting IHCs (Kujawa & Liberman, 2015). However, other changes to cochlear structure may also play a role. Stereocilia and the TM are both intimately involved in the mechanical to electrical transduction performed by cochlear hair cells. This study shows that fusion, elongation, and internalization of stereocilia on IHCs, as well as degeneration and ultimately detachment of the TM from the spiral limbus are consistent features of aging in the inner ear in mice and that identical or similar phenomena occur with aging in humans. These changes can occur without significant loss of OHCs or IHCs. Consequently, the

fusions and elongation of IHC stereocilia and the degeneration of the TM have the potential to be contributors to early age-related decrements in hearing sensitivity.

4.1 | Stereociliary abnormalities in IHCs

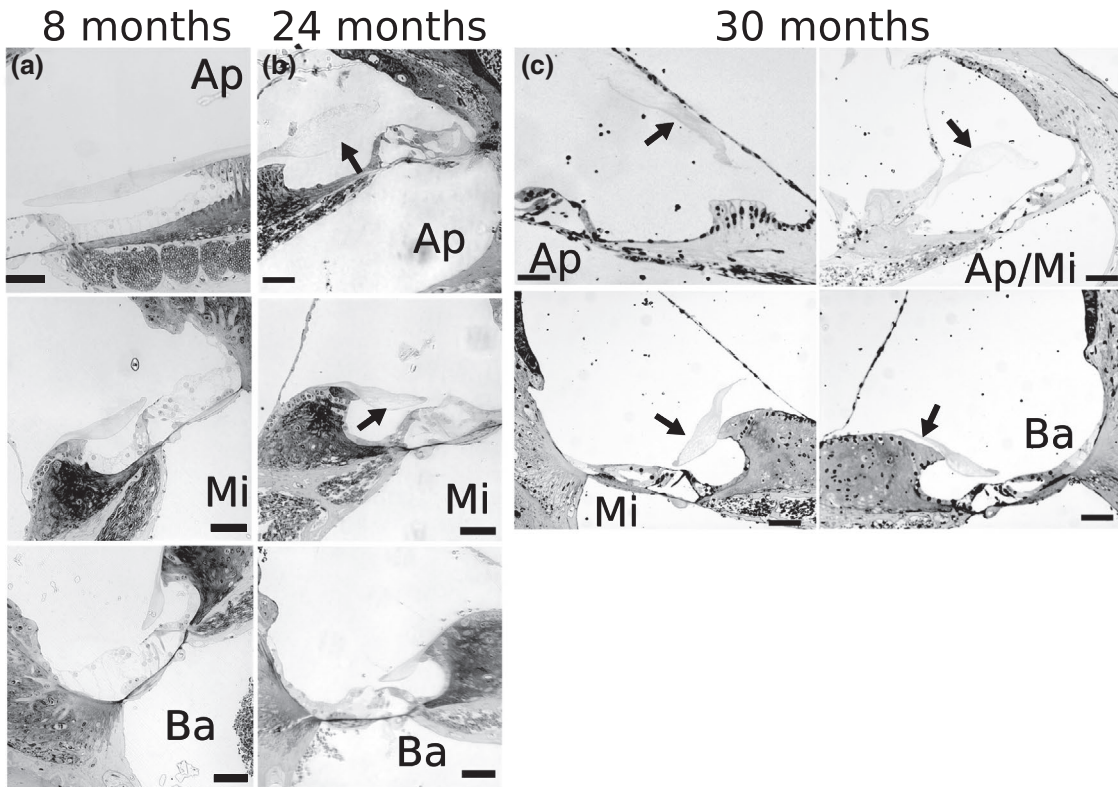
Fusion of stereocilia is likely to affect the transduction of auditory signals by IHCs. Sound-induced movements are detected by stereocilia which pivot at their tapered bottom ends. Deflections alter the tension on “tip-links” that run between the tip of each shorter stereocilium to the shaft the longer stereocilium behind to open and close the mechanotransduction (MET) channels located at the tips of each of the shorter stereocilium, thereby modulating a K⁺ current through the hair cell and therefore its electrical potential (Fettiplace, 2017). Fusion of stereocilia will likely result in a reduced bundle movement due to loss of the taper and increased rigidity of the fused stereocilia due to the incorporation of multiple actin cores. In addition, tip-links will be lost and the number and/or distribution of MET channels may be affected. The result will be loss of signal transduction and the fidelity of sound transmission to the auditory nerve. However, the initial effects of a reduction of the neural output from individual IHC scattered along the organ of Corti to recordable measures of auditory acuity is likely to be subtle and difficult to identify by current methods.

The persistence of stereociliary abnormalities on IHCs, coupled with the absence of indications of damage or degeneration within the body of the IHCs indicate the likelihood of an age-related pathology affecting the hair bundles specifically: a “stereociliopathy.” The stereociliary abnormalities shown in this study are similar to the fusion and elongation of vestibular hair cells described previously (Taylor et al., 2015). This supports the concept that there is a general vulnerability of hair bundle maintenance to the effects of aging in the inner ear. However, while IHCs and vestibular hair cells were strongly affected in both humans and mice, OHCs were not seen to be affected in mice or other rodents (Coleman, 1976; Keithley & Feldman, 1982; Tarnowski et al., 1991) and there were very few

examples of fused stereocilia in OHCs of human samples. This may indicate stereociliary maintenance or deterioration mechanisms vary between different hair cell types.

TEM and the electron tomography show that the paracrystalline arrays of parallel actin filaments are undisturbed when fusion occurs—they do not break, disassemble, or reassociate with each other. Thus,

Mouse



Human

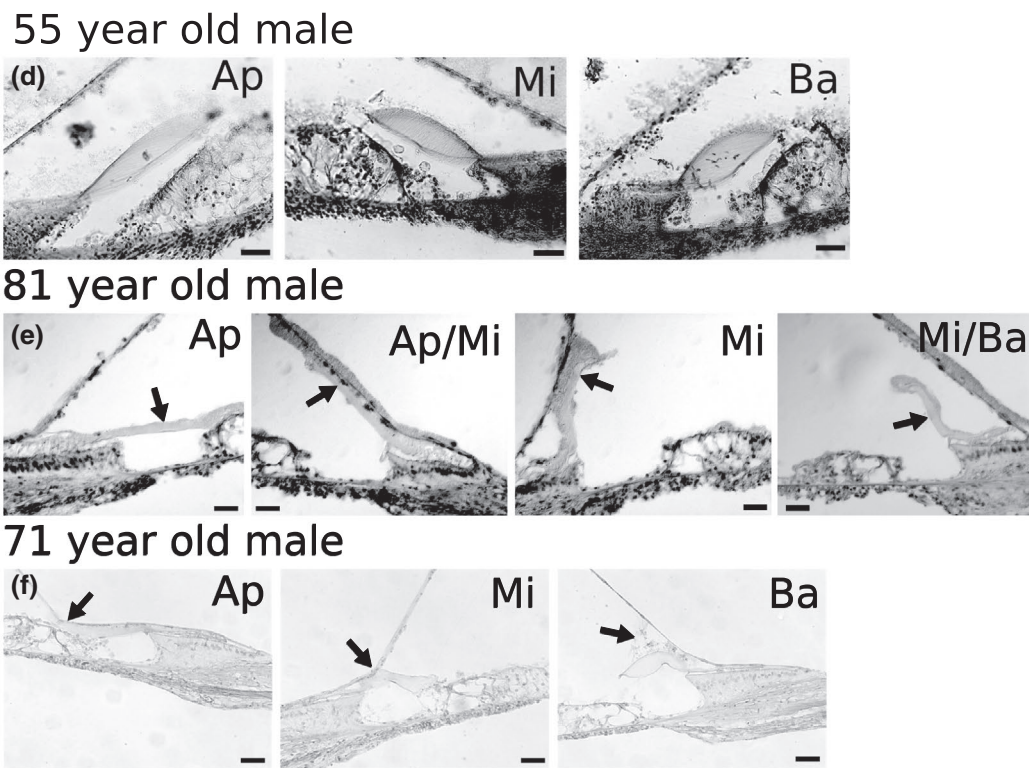


FIGURE 5 Light microscopy of TM degradation in cochleae of aging mice and humans. (a–c) TM structure in mice. (a) 8 months old mouse showing no evidence of degradation in the TM in any coil. (b) 22 months old mouse showing “holes” in the membrane sheet, most severe in the apical coil and not present in the base (black arrows). (c) 30 months old mouse showing detachment of the TM in the apical and middle coils, and evidence of detachment beginning in the basal coil (black arrows); holes in the membrane can also be seen in all three coils. Complete detachment from the spiral limbus and close association with Reissner’s membrane is evident in the apical coil (d–f) TM structure in aging humans. (d) Membrane from a 55 years old male with no recorded hearing loss. Membrane appears as a smooth sheet. (e) In an 81 years old male with reported presbycusis, membrane is thinned throughout the apical and middle coils. The membrane has detached to lie along Reissner’s membrane in the apical and middle coils (black arrows). (f) A second male with presbycusis (71 years old) shows similar thinning of the membrane and attachment to Reissner’s membrane. In the apical and middle coil, the membrane has become attached to Reissner’s membrane, while in the basal coil, although the membrane is not attached, extracellular material can be observed between the tectorial and Reissner’s membranes. Ap, apical coil; Ap/Mid, apical to middle coil; Ba, basal coil; Mi, middle coil. Scale bars: (a–f) = 50 μ m

while the increase in width in fused and giant, elongated stereocilia that subsequently develop is likely a result of accumulation of the existing filaments into the fusing stereocilia, the increase in length is presumably due to growth of the actin filaments. Stereocilia grow in length during development by addition of actin monomers to the apical tips of the filaments and are maintained during life by a slow turnover of actin in a small compartment at that tip (Drummond et al., 2015; McGrath, Roy, & Perrin, 2017; Narayanan et al., 2015; Pelaseyed & Bretscher, 2018). The elongation of stereocilia therefore suggests that the machinery for trafficking actin to the tips of stereocilia is still active, providing additional evidence for the “viability” of the hair cells upon which fused and elongated stereocilia are present. Normally, the precise length of each individual stereocilium is regulated and maintained by a complex of actin capping/depolymerising proteins that are localized to their apical tips (Olt et al., 2014; Peng, Belyantseva, Hsu, Friedman, & Heller, 2009; Zampini et al., 2011). The elongation of stereocilia would seem to imply that regulation is lost, although whether this is because of an age-related reduction in the expression of the relevant proteins, or as a consequence of the effects of membrane fusions on their distribution or density, needs to be assessed.

The electron tomography in this study provides evidence of detachment of the cuticular plate from the apical plasma membrane to form a “gap” of cytoplasm between the membrane and the cuticular plate and the “zipping-up” of detached apical membrane from the base to the tip of the stereocilium to incorporate adjacent bundles into a single fused projection. A similar mechanism for formation of fused stereocilia was suggested in a previous study of aging in vestibular sensory epithelia in mice and humans (Taylor et al., 2015). Membrane inclusions in the apical cytoplasmic space generated by separation of the cuticular plate from the membrane could represent membrane elements trafficked during fusion of stereocilia, which will require membrane remodeling. The role of the microtubules revealed by electron tomography in this region is not known, but may be related to the trafficking of components to or from fusing stereocilia. Vesicles were often present in the cell body region close to the location of internalized actin filament bundles and within the gap that developed between the apical plasma membrane and the cuticular plate, particularly in cells with internalized stereocilia. These vesicles were not seen in younger mice. Many of these vesicles appeared to be double-membraned and similar to autophagic vesicles. This may suggest the actin filaments and other components of the remodeling hair bundle are removed by autophagy. Autophagy acts to remove

damaged or excess cellular material enabling the components to be recycled in support of continuing cellular metabolism and synthesis and is upregulated in times of cellular stress, for example to provide energy sources when cells are starved (and the huge actin content in resorbed stereocilia would make a substantial meal) (Rubinsztein, Marino, & Kroemer, 2011). We have evidence elsewhere that the autophagic flux in IHCs is much greater than that in OHCs (Taylor & Forge, unpublished observation) and it is possible that autophagy plays a role in the prolonged survival of IHCs during aging.

The stereociliopathy observed with aging is similar to that described in a number of conditions thought to result from a defect in the maintenance of actin-cytoskeletal interactions. Fusion and internalization of stereocilia and separation of the cuticular plate from the apical plasma membrane of the hair cell has been observed in mice lacking radixin (Kitajiri et al., 2004), one of the “ERM proteins” (ezrin/radixin/moesin) that act to link actin filaments to the plasma membrane (Fievet, Louvard, & Arpin, 2007). The phenotype develops first in young adults and then progresses but does not result in hair cell loss. Similar stereociliary anomalies are seen in the early postnatal organ of Corti exposed to staurosporine which causes loss of phosphorylated forms of ERM proteins (Goodyear, Ratnayaka, Warchol, & Richardson, 2014). Mutations in the gene encoding myosin 6 also result in fusion and elongation of stereocilia in mice (Self et al., 1999). Here again, the hair bundles show normal characteristics at birth but fusion and elongation occurs subsequently and then progresses in severity and extent into adulthood without any hair cell death occurring. In all these cases, the fusion and internalization of stereocilia appears to occur through detachment and separation of the apical plasma membrane from the cuticular plate and a “zipping-up” of the membrane between the adjacent stereocilia along its length from base to tip, similar to that observed for fusion of stereocilia in the present work. Neither loss of radixin or staurosporine treatment caused hair cell death, and their effects appeared to be specific to the hair bundle. However, both loss of radixin and staurosporine exposure cause apparently similar effects on both IHCs and OHCs, but radixin loss affects only cochlear hair cells and not those of the vestibular system (Kitajiri et al., 2004). Myosin 6 may have several roles in the hair cell, but the finding of apical membrane detachment in the early stages of the fusion process suggested the likelihood that myosin 6 acts to anchor the apical plasma membrane to the cuticular plate and possibly also maintain membrane domain composition.

Stereocilia fusion and elongation are also associated with mutations in PTPRQ, a receptor-like inositol lipid phosphatase, required for formation during development of "shaft connectors" that form

links between the membranes of adjacent stereocilia. Its absence results in fused-elongated stereocilia in IHCs of the mature organ of Corti (Goodyear et al., 2003). It could be hypothesized that

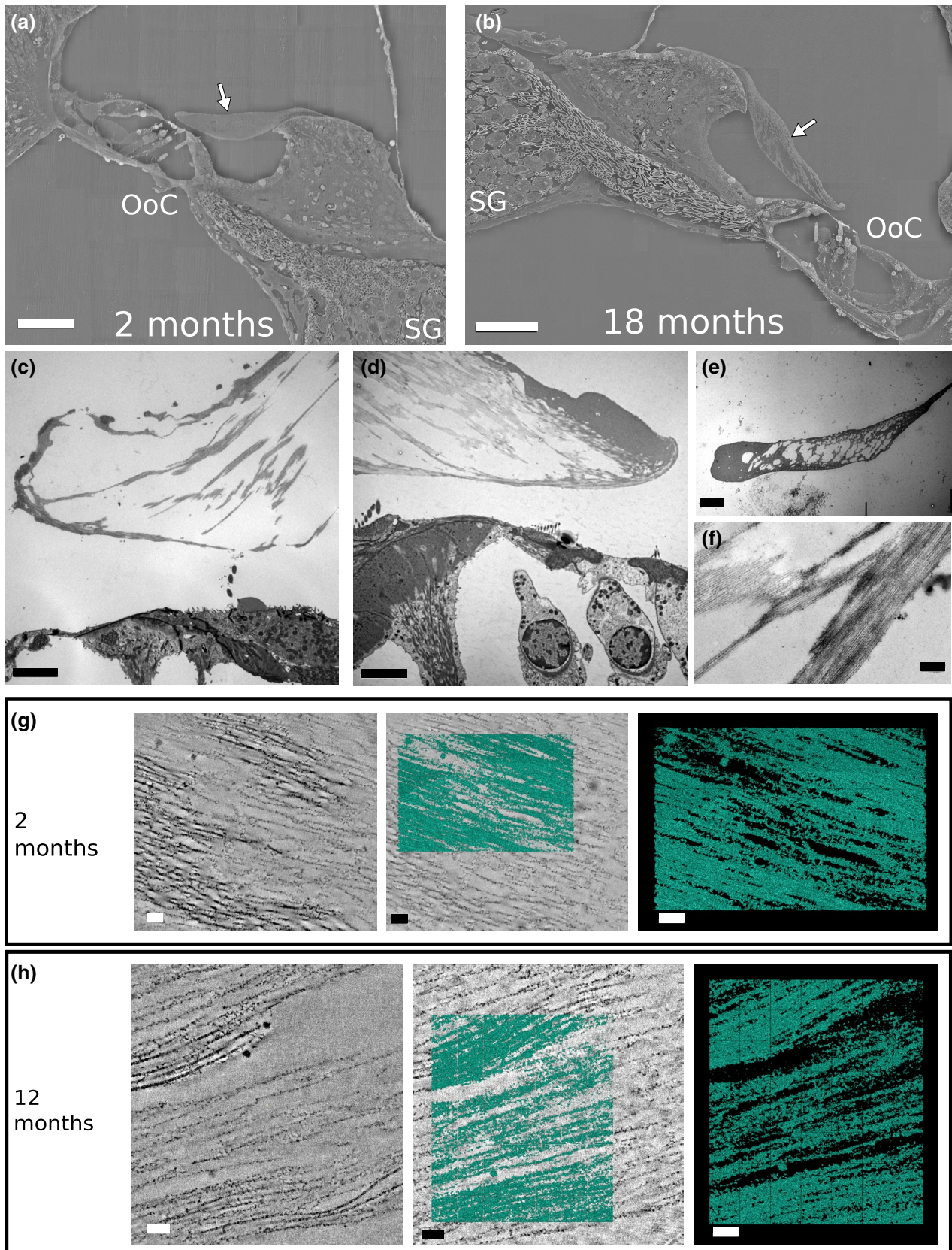


FIGURE 6 TM matrix degradation in aging mice. (a–b) Backscatter imaging of resin sections showing middle turn in (a) 2 months and (b) 18 months mice. TM (white arrows) in (b) shows the same thinning and holes apparent by light microscopy. The structure of the organ of Corti (OoC) shows no obvious defects and there is no obvious loss of cell bodies in the spiral ganglion (SG). (c–f) TEM imaging of TM in 24 months old mice. (c) Very little striated-sheet matrix remains leaving only the remains of the collagen skeleton. (d) In some samples although the matrix was lost, other structural elements around the periphery of the TM were intact. (e) Thinning of the membrane was also observed in mice. (f) High resolution shows the presence of collagen skeleton with loss of the matrix. (g–h) Electron tomography of the TM in 2 months (g) and 12 months old mice (h). By 12 months, larger spaces are appearing in the striated-sheet matrix, suggesting matrix material has been lost. Scale bars: a–b = 50 μ m, c–e = 5 μ m, f = 500 nm, g–h = 100 nm. For model rotations see Supporting Information Movies S2 and S3

fusion occurs when membranes of adjacent stereocilia come into contact and that loss of PTPRQ and consequently shaft connectors might therefore facilitate fusion. However, loss of shaft connectors in PTPRQ mutants does not lead to direct contact of adjacent stereocilia (Goodyear et al., 2003). PTPRQ may act to regulate and maintain local inositol phosphoinositide phospholipid composition, in turn regulating the rates of membrane and actin turnover. Consequently, loss of PTPRQ would result in failure to maintain stereociliary membrane domain composition and associated membrane–cytoskeletal interactions, facilitating fusion events. There is evidence that there are differences between hair cell types in their susceptibility to loss of PTPRQ possibly because in some hair cell types other phosphatases can compensate for its loss (Goodyear et al., 2003). This could be a factor underlying the observed difference between IHCs and OHCs in age-related stereociliary “fusion-competence.”

Although the molecular and biochemical mechanisms at work during the age-related stereociliopathy are not clear, similarities with the effects of inactivation of ERM proteins, loss of myosin 6, and PTPRQ mutations indicate that an age-related failure to maintain regulation of membrane turnover and membrane–cytoskeletal interactions within the stereocilia may be a significant factor in stereociliopathy. The stereociliopathies described here appeared scattered along the cochlear spiral, although there was some evidence that giant stereocilia may be more common at the apex of the cochlea compared to the base. The reason for this potential apex to base gradient is not clear, although it may indicate differences in stereociliary maintenance and actin turnover along the length of the cochlea.

4.2 | TM degeneration

In addition to stereociliopathy, age-related degradation of the TM has also been identified in this study as a potential contributor to hearing deficits in humans. Recent work has shown a similar TM phenotype in aging of several wild-type mouse strains, and indicated that the severity of aging phenotype may be genetically determined (Goodyear et al., 2019). The TM performs several tasks (Goodyear & Richardson, 2018; Lukashkin, Richardson, & Russell, 2010), but primarily maximizes the sound-induced movement that deflects IHC stereocilia at their best or characteristic frequency. The TM is therefore responsible for enhancing both the auditory sensitivity and frequency selectivity. TM function depends upon

its physical properties, its mass and its stiffness, both of which vary systematically along the cochlea—mass increases from base to apex; stiffness increases apex to base (Goodyear & Richardson, 2018; Teudt & Richter, 2014). Our study reveals in mice a progressive degeneration of the TM that will affect its physical properties, proceeding with increasing age from the apical coils toward the base. This is apparent initially as a progressive loss of the striated-sheet matrix and the two major glycoproteins of which it composed, TECTA and TECTB (Goodyear & Richardson, 2018), that proceeds from the central regions of the membrane toward the periphery. “Holes” appear in the body of TM and there is a subsequent decrease in density of the radial collagen fibrils, such that in some of the oldest animals the TM may appear as little more than an “exoskeleton” surrounding a significantly reduced density of collagen fibrils. Beginning in the apical coil, the TM separates from the spiral limbus eventually detaching completely and becoming associated with the endolymphatic side of Reissner’s membrane. During the progressive degeneration TM shape changes, sometimes appearing thinned and sometimes apparently swollen. Changes in the shape of the TM suggesting the changes in composition, in particular thinning of the membrane, as well as evidence of separation from the spiral limbus and close association or attachment with the Reissner’s membrane, were also evident in the cochleae of older human subjects. Although the TM remained in proximity to the hair cells at the very apex of the human cochleae studied, the thinning and attachment to Reissner’s membrane were most pronounced in the apical and middle coils, suggesting the possibility that an age-related apical to basal progression of TM disruption along the organ of Corti, similar to that seen in mice, may also occur in humans.

TECTA and TECTB are produced only for a short time during early development (Rau, Legan, & Richardson, 1999), and the matrix is not replenished during life. CEACAM16, which interacts with both TECTA and TECTB and is required for striated-sheet formation, is produced throughout life. (Cheatham et al., 2014). Targeted deletion of the genes encoding TECTA (*Tecta*) (Legan et al., 2000) and TECTB (*Tectb*) (Russell et al., 2007) induces loss of the striated-sheet matrix and hearing impairment, without any effects on hair cells. Non-syndromic autosomal hearing loss in humans results from point mutations in the human homolog for TECTA (*TECTA*) that are either dominant (DFNA8/12) or recessive (DFNB21) and likewise for CEACAM16 (DFNA4b and DFNB113). With loss of TECTA, TECTB is also lost. Morphologically, the TM appears less dense than normal, its shape is disrupted and it

separates from the spiral limbus, detaching completely to become closely associated with Reissner's membrane. Point mutations in *Tecta* in mice cause elevation of auditory thresholds, although the different mutations result in distinctive disruptions of particular

details of TM structure. Shape changes and reduction in the zone of attachment with the spiral limbus were common features, and in some the reduced *TECTB* expression and advanced detachment of the TM were particularly pronounced in apical coils (Legan et

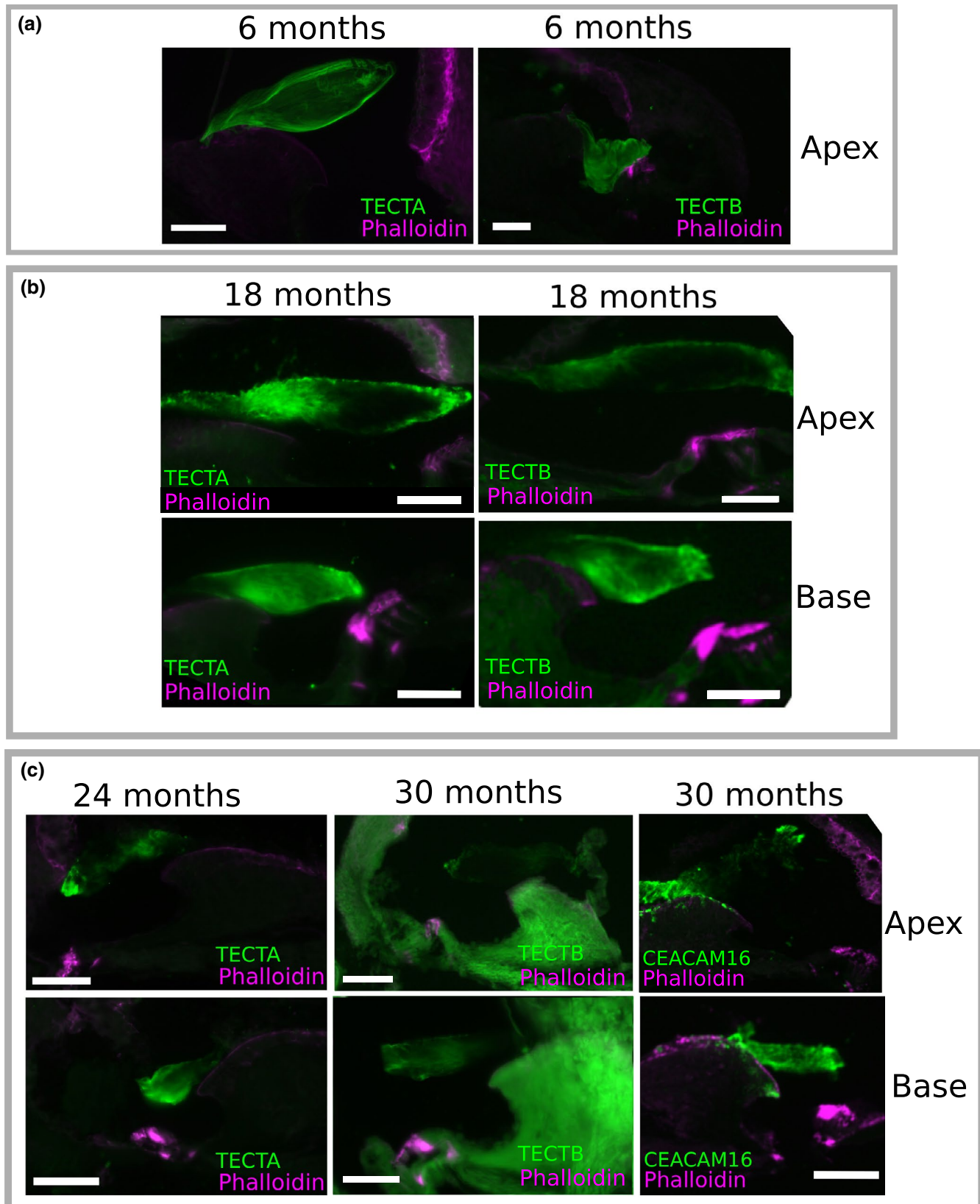


FIGURE 7 Immunohistochemistry of striated-sheet matrix proteins in aging mouse cochleae. Three striated-sheet matrix proteins were stained by immunohistochemistry (green). (a) TECTA and TECTB labeling at 6 months in the mouse cochlear apex. Strong labeling is shown consistently across the TM. (b) TECTA and TECTB labeling at 18 months in the apex and base of the mouse cochlea. At the apex, TECTA and TECTB have been lost from the centre of the TM but persists at the periphery. At the base, staining for both proteins is consistent at 18 months and has just begun to fade at the centre for TECTB. (c) TECTA, TECTB, and CEACAM16 labeling at the apex and base of the mouse cochlea at 24–30 months. All three proteins have been lost from the centre of the TM in the cochlear apex. There is some evidence of loss of TECTA and TECTB in the centre of the TM at the cochlear base, although CEACAM16 staining is more consistent. All samples were counterstained with phalloidin (magenta) to identify the actin in the organ of Corti. Scale bars: 50 μ m

al., 2014). Loss of TECTB also results in loss of the striated-sheet matrix, and large changes in TM cross-sectional profile in the apical coil causing a loss of low-frequency hearing. However TECTA is still expressed in the *Tectb*^{-/-} mice and the TM does not detach from the spiral limbus. Detailed analysis of the biophysical and physiological consequences of loss of TECTB suggests it is essential for low-frequency hearing (Russell et al., 2007). Levels of TECTB, but not of TECTA, are slightly reduced in the TM of mice carrying a targeted null mutation in *Ceacam16*. In these mice, the TM remains attached to spiral limbus, but there are "holes" within the body of the TM that are most pronounced in the apical coils (Cheatham et al., 2014) and similar to those seen in the much older wild-type mice used in the current study. Recent work has also shown that CEACAM16 is required to maintain the TM structure during aging, and that its absence produces an accelerated aging phenotype (Goodyear et al., 2019).

It is also possible that an age-related reduction in endocochlear potential (EP) and degeneration of the stria vascularis may affect TM structure. The TM is sensitive to its ionic environment, particularly calcium concentration (Goodyear & Richardson, 2018; Strimbu, Prasad, Hakizimana, & Fridberger, 2019). However, the stria vascularis is primarily responsible for maintaining potassium ions and EP (Salt, Melichar, & Thalmann, 1987), and how this affects overall ion balance in endolymph is not clear. It is therefore difficult to speculate on whether there are changes in the ionic environment of the endolymph in which the TM is bathed contribute in any way to the degeneration observed, and this was not studied in these experiments.

Therefore, it is possible to hypothesize two scenarios leading to the age-related degeneration of the TM. Both immunohistochemistry and the detachment of the TM from the spiral limbus in both mice and humans strongly suggests that loss of TECTA is a significant factor in age-related TM degradation. This could suggest that tectorins are the principle target of degradation, as these proteins are not replenished throughout life. A second hypothesis is that CEACAM16 acts as a stabilizer for the tectorin proteins in the striated-sheet matrix, and it is a reduction or dysregulation of the production of this protein with aging that leads to degradation of the matrix and loss of the tectorin proteins. Late-onset hearing loss is also present in humans with mutations in CEACAM16 (DFNB113) indicating that this may be an important factor in age-related TM degradation and hearing loss (Goodyear et al., 2019).

This study was limited in its human data by the limited number of samples of sufficient quality and with appropriate medical history that

could be included (i.e., the presence or known absence of presbycusis in the older samples). However, despite this we were able to demonstrate stereociliary fusion phenotypes in both sexes, although we only had suitable TM examples from males. Due to these limitations, it is difficult to say if there were any sex differences between the samples as sample numbers are not sufficient. In the mouse studies, male mice were used exclusively, to avoid confounding factors from the different rates of ARHL between the sexes (Guimaraes et al., 2004). This does mean the study is limited in examining the potential sex differences in these phenotypes. Such differences may well-exist, given the differing rates of ARHL between the sexes in mice, and the description of these phenotypes in this study could form the basis of a future examination of this question.

Age-related increases of auditory thresholds are typically reported as beginning at high frequencies progressing to involve successively lower frequencies, broadly corresponding to progressive loss of OHCs proceeding from the basal coil apicalwards. Age-related synaptopathies are reported to occur in an apex to base pattern (Sergeyenko et al., 2013), similar to the patterns of stereociliopathy and TM degradation reported here. In particular, the pattern of occurrence of TM deterioration observed here suggests the likelihood of a low-frequency component in the early stages of ARHL and which may be contributing to the so-called "hidden hearing loss." The continued deterioration progressing toward the base without obvious loss of hair cells could also suggest that TM degeneration contributes to age-related threshold elevations. The combination of all these factors is therefore likely to contribute to the early and later stages of ARHL. This raises important questions for the development of future therapies, which must contend not only with hair cell loss and synaptopathy but also with hair cells that are present but whose function is impaired, and with the potential need to regenerate the TM. Therefore future therapeutic approaches may require a holistic approach to the organ of Corti and its surrounding structures to maximize their effectiveness.

DECLARATION OF TRANSPARENCY

The authors, reviewers, and editors affirm that in accordance with the policies set by the *Journal of Neuroscience Research* this manuscript presents an accurate and transparent account of the study being reported and that all critical details describing the methods and results are present.

ACKNOWLEDGMENTS

The authors thank Lucy Anderson for kindly providing some of the samples used in this study, Graham Nevill for technical assistance in sample preparation, and Katie Smith for sample preparation and imaging.

CONFLICT OF INTEREST

Authors have no known conflict of interest to declare.

AUTHOR CONTRIBUTIONS

AB, AF, and RT had full access to all the data in the study and take responsibility for the integrity of the data and the accuracy of the data analysis. *Conceptualization*, A.B., A.F., R.G., G.R., R.T., and T.W.; *Methodology*, A.B., A.F., R.T., and T.W.; *Investigation*, A.B., A.F., R.T., and T.W.; *Resources*, A.B., A.F., R.G., G.R., R.T., and T.W.; *Writing – Original Draft*, A.B., A.F., and R.T.; *Writing – Review & Editing*, A.B., A.F., R.G., G.R., R.T., and T.W.; *Visualization*, A.B. and A.F.; *Funding Acquisition*, A.F., R.T., and A.B.

ORCID

Anwen Bullen  <https://orcid.org/0000-0002-6705-5263>

Andrew Forge  <https://orcid.org/0000-0002-0995-0219>

Guy P. Richardson  <https://orcid.org/0000-0001-8476-0223>

Richard J. Goodyear  <https://orcid.org/0000-0001-6698-4127>

Ruth Taylor  <https://orcid.org/0000-0001-7359-1604>

DATA AVAILABILITY STATEMENT

Data available on request from the authors. Ethical and privacy restrictions may apply to human data.

REFERENCES

- Bao, J., & Ohlemiller, K. K. (2010). Age-related loss of spiral ganglion neurons. *Hearing Research*, 264, 93–97.
- Barbee, C. M., James, J. A., Park, J. H., Smith, E. M., Johnson, C. E., Clifton, S., & Danhauer, J. L. (2018). Effectiveness of auditory measures for detecting hidden hearing loss and/or cochlear synaptopathy: A systematic review. *Seminars in Hearing*, 39, 172–209.
- Bullen, A. (2019). The automatic tape collection ultramicrotome (ATUM). In R. A. Fleck & B. M. Humbel (Eds.), *Biological field emission scanning electron microscopy* (pp. 485–494). Chichester, UK: Wiley.
- Cheatham, M. A., Goodyear, R. J., Homma, K., Legan, P. K., Korchagina, J., Naskar, S., ... Richardson, G. P. (2014). Loss of the tectorial membrane protein CEACAM16 enhances spontaneous, stimulus-frequency, and transiently evoked otoacoustic emissions. *Journal of Neuroscience*, 34, 10325–10338.
- Coleman, J. W. (1976). Hair cell loss as a function of age in the normal cochlea of the guinea pig. *Acta Oto-Laryngologica*, 82, 33–40.
- Davies, S., & Forge, A. (1987). Preparation of the mammalian organ of Corti for scanning electron microscopy. *Journal of Microscopy*, 147, 89–101.
- Davis, A. (1995). *Hearing in adults: The prevalence and distribution of hearing impairment and reported hearing disability in the MRC Institute of Hearing Research's National Study of Hearing*. London, UK: Whurr Publishers Ltd.
- Drummond, M. C., Barzik, M., Bird, J. E., Zhang, D. S., Lechene, C. P., Corey, D. P., ... Friedman, T. B. (2015). Live-cell imaging of actin dynamics reveals mechanisms of stereocilia length regulation in the inner ear. *Nature Communications*, 6, 6873.
- Engle, J. R., Tinling, S., & Recanzone, G. H. (2013). Age-related hearing loss in rhesus monkeys is correlated with cochlear histopathologies. *PLoS One*, 8, e55092.
- Fettiplace, R. (2017). Hair cell transduction, tuning, and synaptic transmission in the mammalian cochlea. *Comprehensive Physiology*, 7, 1197–1227.
- Fievet, B., Louvard, D., & Arpin, M. (2007). ERM proteins in epithelial cell organization and functions. *Biochimica et Biophysica Acta*, 1773, 653–660. <https://doi.org/10.1016/j.bbamcr.2006.06.013>
- Gleich, O., Semmler, P., & Strutz, J. (2016). Behavioral auditory thresholds and loss of ribbon synapses at inner hair cells in aged gerbils. *Experimental Gerontology*, 84, 61–70. <https://doi.org/10.1016/j.exger.2016.08.011>
- Goodyear, R. J., Cheatham, M. A., Naskar, S., Zhou, Y., Osgood, R. T., Zheng, J., & Richardson, G. P. (2019). Accelerated age-related degradation of the tectorial membrane in the Ceacam16 β -gal/ β -gal null mutant mouse, a model for late-onset human hereditary deafness DFNB113. *Frontiers in Molecular Neuroscience*, 12, 147.
- Goodyear, R. J., Legan, P. K., Wright, M. B., Marcotti, W., Oganesian, A., Coats, S. A., ... Richardson, G. P. (2003). A receptor-like inositol lipid phosphatase is required for the maturation of developing cochlear hair bundles. *Journal of Neuroscience*, 23, 9208–9219. <https://doi.org/10.1523/JNEUROSCI.23-27-09208.2003>
- Goodyear, R. J., Rathnayaka, H. S., Warchol, M. E., & Richardson, G. P. (2014). Staurosporine-induced collapse of cochlear hair bundles. *Journal of Comparative Neurology*, 522, 3281–3294. <https://doi.org/10.1002/cne.23597>
- Goodyear, R. J., & Richardson, G. P. (2002). Extracellular matrices associated with the apical surfaces of sensory epithelia in the inner ear: Molecular and structural diversity. *Journal of Neurobiology*, 53, 212–227. <https://doi.org/10.1002/neu.10097>
- Goodyear, R. J., & Richardson, G. P. (2018). Structure, function, and development of the tectorial membrane: An extracellular matrix essential for hearing. *Current Topics in Developmental Biology*, 130, 217–244.
- Gratton, M. A., Schmidt, R. A., & Schulte, B. A. (1996). Age-related decreases in endocochlear potential are associated with vascular abnormalities in the stria vascularis. *Hearing Research*, 102, 181–190. [https://doi.org/10.1016/S0378-5955\(96\)90017-9](https://doi.org/10.1016/S0378-5955(96)90017-9)
- Guimaraes, P., Zhu, X., Cannon, T., Kim, S., & Frisina, R. D. (2004). Sex differences in distortion product otoacoustic emissions as a function of age in CBA mice. *Hearing Research*, 192, 83–89. <https://doi.org/10.1016/j.heares.2004.01.013>
- Hasko, J. A., & Richardson, G. P. (1988). The ultrastructural organization and properties of the mouse tectorial membrane matrix. *Hearing Research*, 35, 21–38. [https://doi.org/10.1016/0378-5955\(88\)90037-8](https://doi.org/10.1016/0378-5955(88)90037-8)
- Hequembourg, S., & Liberman, M. C. (2001). Spiral ligament pathology: A major aspect of age-related cochlear degeneration in C57BL/6 mice. *Journal of the Association for Research in Otolaryngology*, 2, 118–129. <https://doi.org/10.1007/s101620010075>
- Ichimiya, I., Suzuki, M., & Mogi, G. (2000). Age-related changes in the murine cochlear lateral wall. *Hearing Research*, 139, 116–122. [https://doi.org/10.1016/S0378-5955\(99\)00170-7](https://doi.org/10.1016/S0378-5955(99)00170-7)
- Keithley, E. M., & Feldman, M. L. (1982). Hair cell counts in an age-graded series of rat cochleas. *Hearing Research*, 8, 249–262. [https://doi.org/10.1016/0378-5955\(82\)90017-X](https://doi.org/10.1016/0378-5955(82)90017-X)
- Kitajiri, S., Fukumoto, K., Hata, M., Sasaki, H., Katsuno, T., Nakagawa, T., ... Tsukita, S. (2004). Radixin deficiency causes deafness associated with progressive degeneration of cochlear stereocilia. *Journal of Cell Biology*, 166, 559–570. <https://doi.org/10.1083/jcb.200402007>
- Knipper, M., Richardson, G., Mack, A., Muller, M., Goodyear, R., Limberger, A., ... Zimmermann, U. (2001). Thyroid hormone-deficient period prior to the onset of hearing is associated with reduced levels of β -tectorin protein in the tectorial membrane: Implication for hearing loss. *Journal of Biological Chemistry*, 276, 39046–39052.

- Kremer, J. R., Mastronarde, D. N., & McIntosh, J. R. (1996). Computer visualization of three-dimensional image data using IMOD. *Journal of Structural Biology*, 116, 71–76. <https://doi.org/10.1006/jbsb.1996.0013>
- Kujawa, S. G., & Liberman, M. C. (2015). Synaptopathy in the noise-exposed and aging cochlea: Primary neural degeneration in acquired sensorineural hearing loss. *Hearing Research*, 330, 191–199. <https://doi.org/10.1016/j.heares.2015.02.009>
- Kusunoki, T., Cureoglu, S., Schachern, P. A., Baba, K., Kariya, S., & Paparella, M. M. (2004). Age-related histopathologic changes in the human cochlea: A temporal bone study. *Otolaryngology-Head and Neck Surgery*, 131, 897–903. <https://doi.org/10.1016/j.otohns.2004.05.022>
- Legan, P. K., Goodear, R. J., Morin, M., Mencia, A., Pollard, H., Olavarrieta, L., ... Richardson, G. P. (2014). Three deaf mice: Mouse models for TECTA-based human hereditary deafness reveal domain-specific structural phenotypes in the tectorial membrane. *Human Molecular Genetics*, 23, 2551–2568. <https://doi.org/10.1093/hmg/ddt646>
- Legan, P. K., Lukashkina, V. A., Goodear, R. J., Kossi, M., Russell, I. J., & Richardson, G. P. (2000). A targeted deletion in α -tectorin reveals that the tectorial membrane is required for the gain and timing of cochlear feedback. *Neuron*, 28, 273–285.
- Lukashkin, A. N., Richardson, G. P., & Russell, I. J. (2010). Multiple roles for the tectorial membrane in the active cochlea. *Hearing Research*, 266, 26–35.
- McGrath, J., Roy, P., & Perrin, B. J. (2017). Stereocilia morphogenesis and maintenance through regulation of actin stability. *Seminars in Cell & Developmental Biology*, 65, 88–95.
- Narayanan, P., Chatterton, P., Ikeda, A., Ikeda, S., Corey, D. P., Ervasti, J. M., & Perrin, B. J. (2015). Length regulation of mechanosensitive stereocilia depends on very slow actin dynamics and filament-severing proteins. *Nature Communications*, 6, 6855.
- Olt, J., Mburu, P., Johnson, S. L., Parker, A., Kuhn, S., Bowl, M., ... Brown, S. D. M. (2014). The actin-binding proteins Eps8 and gelsolin have complementary roles in regulating the growth and stability of mechanosensory hair bundles of mammalian cochlear outer hair cells. *PLoS One*, 9, e87331.
- Parthasarathy, A., & Kujawa, S. G. (2018). Synaptopathy in the aging cochlea: Characterizing early-neuronal deficits in auditory temporal envelope processing. *Journal of Neuroscience*, 38, 7108–7119.
- Pelaseyed, T., & Bretscher, A. (2018). Regulation of actin-based apical structures on epithelial cells. *Journal of Cell Science*, 131:jcs221853.
- Peng, A. W., Belyantseva, I. A., Hsu, P. D., Friedman, T. B., & Heller, S. (2009). Twinfilin 2 regulates actin filament lengths in cochlear stereocilia. *Journal of Neuroscience*, 29, 15083–15088.
- Rau, A., Legan, P. K., & Richardson, G. P. (1999). Tectorin mRNA expression is spatially and temporally restricted during mouse inner ear development. *Journal of Comparative Neurology*, 405, 271–280.
- Rauch, S. D., Velazquez-Villasenor, L., Dimitri, P. S., & Merchant, S. N. (2001). Decreasing hair cell counts in aging humans. *Annals of the New York Academy of Sciences*, 942, 220–227.
- Rubinsztein, D. C., Marino, G., & Kroemer, G. (2011). Autophagy and aging. *Cell*, 146, 682–695.
- Russell, I. J., Legan, P. K., Lukashkina, V. A., Lukashkin, A. N., Goodear, R. J., & Richardson, G. P. (2007). Sharpened cochlear tuning in a mouse with a genetically modified tectorial membrane. *Nature Neuroscience*, 10, 215–223. <https://doi.org/10.1038/nn1828>
- Salt, A. N., Melichar, I., & Thalmann, R. (1987). Mechanisms of endocochlear potential generation by stria vascularis. *Laryngoscope*, 97, 984–991. <https://doi.org/10.1288/00005537-198708000-00020>
- Schmiedt, R. A. (1996). Effects of aging on potassium homeostasis and the endocochlear potential in the gerbil cochlea. *Hearing Research*, 102, 125–132. [https://doi.org/10.1016/S0378-5955\(96\)00154-2](https://doi.org/10.1016/S0378-5955(96)00154-2)
- Schmiedt, R. A., Mills, J. H., & Boettcher, F. A. (1996). Age-related loss of activity of auditory-nerve fibers. *Journal of Neurophysiology*, 76, 2799–2803. <https://doi.org/10.1152/jn.1996.76.4.2799>
- Self, T., Sobe, T., Copeland, N. G., Jenkins, N. A., Avraham, K. B., & Steel, K. P. (1999). Role of myosin VI in the differentiation of cochlear hair cells. *Developmental Biology*, 214, 331–341. <https://doi.org/10.1006/dbio.1999.9424>
- Sergeyenko, Y., Lall, K., Liberman, M. C., & Kujawa, S. G. (2013). Age-related cochlear synaptopathy: An early-onset contributor to auditory functional decline. *Journal of Neuroscience*, 33, 13686–13694. <https://doi.org/10.1523/JNEUROSCI.1783-13.2013>
- Strimbu, C. E., Prasad, S., Hakizimana, P., & Fridberger, A. (2019). Control of hearing sensitivity by tectorial membrane calcium. *Proceedings of the National Academy of Sciences of the United States of America*, 116, 5756–5764. <https://doi.org/10.1073/pnas.1805223116>
- Suzuki, T., Nomoto, Y., Nakagawa, T., Kuwahata, N., Ogawa, H., Suzuki, Y., ... Omori, K. (2006). Age-dependent degeneration of the stria vascularis in human cochleae. *Laryngoscope*, 116, 1846–1850. <https://doi.org/10.1097/01.mlg.0000234940.33569.39>
- Tarnowski, B. I., Schmiedt, R. A., Hellstrom, L. I., Lee, F. S., & Adams, J. C. (1991). Age-related changes in cochleas of mongolian gerbils. *Hearing Research*, 54, 123–134. [https://doi.org/10.1016/0378-5955\(91\)90142-V](https://doi.org/10.1016/0378-5955(91)90142-V)
- Taylor, R. R., Jagger, D. J., Saeed, S. R., Axon, P., Donnelly, N., Tysome, J., ... Forge, A. (2015). Characterizing human vestibular sensory epithelia for experimental studies: New hair bundles on old tissue and implications for therapeutic interventions in ageing. *Neurobiology of Aging*, 36, 2068–2084. <https://doi.org/10.1016/j.neurobiaging.2015.02.013>
- Teudt, I. U., & Richter, C. P. (2014). Basilar membrane and tectorial membrane stiffness in the CBA/CaJ mouse. *Journal of the Association for Research in Otolaryngology*, 15, 675–694. <https://doi.org/10.1007/s10162-014-0463-y>
- Thomopoulos, G. N., Spicer, S. S., Gratton, M. A., & Schulte, B. A. (1997). Age-related thickening of basement membrane in stria vascularis capillaries. *Hearing Research*, 111, 31–41. [https://doi.org/10.1016/S0378-5955\(97\)00080-4](https://doi.org/10.1016/S0378-5955(97)00080-4)
- Wright, A. (1982). Giant cilia in the human organ of Corti. *Clinical Otolaryngology & Allied Sciences*, 7, 193–199. <https://doi.org/10.1111/j.1365-2273.1982.tb01582.x>
- Wright, A. (1984). Dimensions of the cochlear stereocilia in man and the guinea pig. *Hearing Research*, 13, 89–98. [https://doi.org/10.1016/0378-5955\(84\)90099-6](https://doi.org/10.1016/0378-5955(84)90099-6)
- Wright, A., Davis, A., Bredberg, G., Ulehlova, L., & Spencer, H. (1987). Hair cell distributions in the normal human cochlea. *Acta Otolaryngologica Supplementum*, 444, 1–48.
- Wu, P. Z., Liberman, M. D., Bennett, K., de Gruttola, V., O'Malley, J. T., & Liberman, M. C. (2018). Primary neural degeneration in the human cochlea: Evidence for hidden hearing loss in the aging ear. *Neuroscience*, 407, 8–20. <https://doi.org/10.1016/j.neuroscience.2018.07.053>
- Yamasoba, T., Someya, S., Yamada, C., Weindruch, R., Prolla, T. A., & Tanokura, M. (2007). Role of mitochondrial dysfunction and mitochondrial DNA mutations in age-related hearing loss. *Hearing Research*, 226, 185–193. <https://doi.org/10.1016/j.heares.2006.06.004>
- Zampini, V., Ruttiger, L., Johnson, S. L., Franz, C., Furness, D. N., Waldhaus, J., ... Marcotti, W. (2011). Eps8 regulates hair bundle length and functional maturation of mammalian auditory hair cells. *PLoS Biology*, 9, e1001048. <https://doi.org/10.1371/journal.pbio.1001048>
- Zheng, J., Miller, K. K., Yang, T., Hildebrand, M. S., Shearer, A. E., DeLuca, A. P., ... Dallos, P. (2011). Carcinoembryonic antigen-related cell adhesion molecule 16 interacts with α -tectorin and is mutated in autosomal dominant hearing loss (DFNA4). *Proceedings of the National Academy of Sciences of the United States of America*, 108, 4218–4223.

SUPPORTING INFORMATION

Additional supporting information may be found online in the Supporting Information section.

Movie S1. Reconstruction and model of stereociliary fusion electron tomography from 1 year old mouse

Movie S2 and S3. Reconstruction and models of tectorial membrane matrix in 2 and 12 months mice

Transparent Peer Review Report

Transparent Science Questionnaire for Authors

How to cite this article: Bullen A, Forge A, Wright A, Richardson GP, Goodyear RJ, Taylor R. Ultrastructural defects in stereocilia and tectorial membrane in aging mouse and human cochleae. *J Neuro Sci.* 2019;00:1-19. <https://doi.org/10.1002/jnr.24556>